Incompressible Irrotational Axisymmetric Flow about a Body of Revolution: The Inverse Problem

M. Fouad Zedan* and Charles Dalton†
University of Houston, Houston, Texas

The flow of an incompressible fluid past an axisymmetric shape is considered in the form of the "inverse problem" in hydrodynamics. For a given pressure or velocity distribution, the appropriate body shape is determined iteratively. The method of line sources and sinks is used to represent the body shape. The procedure is simple and accurate and convergence is more rapid than that obtained by other investigators using surface-source distributions. Examples chosen to represent the method include spheres, Rankine bodies, a constant velocity body, and an airfoil-shape axisymmetric body. Results compare very well with exact solutions and with calculated results of others when comparison is possible.

I. Introduction

IN the design of optimum aerodynamic shapes for incompressible flow, minimization of the drag is an important requirement. If no separation occurs, most of the drag is caused by skin friction. The skin friction is computed from the boundary-layer solution, which is determined from the velocity distribution outside the boundary layer. Previous studies have shown that the external flow velocity distribution is close to that predicted by potential flow provided that no separation occurs.

In potential flow there are two basic approaches to body shape design; these are known as the "direct problem" and the "inverse problem." In the direct problem, the body geometry is prescribed, whereas the flowfield is required. For the inverse problem, the objective is to determine the body geometry corresponding to a given surface distribution of velocity or pressure. The solution of the direct problem generally is easier than the inverse problem. The direct problem can be considered to be completely solved even for complicated three-dimensional bodies and flow situations, as will be shown in Sec. II. As for the inverse problem; some success was achieved in two-dimensional flow because of the availability of complex variables and conformal mapping techniques, whereas no successful method was available in three-dimensional flow, except a method developed recently by Bristow.[1] Although the method is limited to axisymmetric flow, it is tedious and requires lengthy calculations.

Clearly, the inverse problem is much more desirable in designing optimum aerodynamic shapes, since one can input a velocity distribution that is known to have desirable features (noncavitating, nonseparating, low drag...etc.), and then obtain the corresponding body. This means tremendous saving in time and effort as compared to solving the direct problem for a number of shapes, and choosing the one that provides the desired features.

In this paper, a method for solving the inverse problem in axisymmetric flow is presented. The method is simple, fast, and yet still accurate enough for most practical purposes, as shown by the numerous test cases.

Received March 3, 1977; revision received May 7, 1977; presented as Paper 77-1175 at the AIAA Lighter-than-Air-Systems Technology Conference, Melbourne, Fla., Aug. 11-12, 1977 (in bound volume of Conference Papers).

Index categories: Aerodynamics; Lighter-than-Airships; Hydrodynamics.

*Doctoral Candidate, Department of Mechanical Engineering.

†Associate Professor, Department of Mechanical Engineering. Member AIAA.

II. Previous Studies

The direct problem has been treated by numerous studies for a wide variety of body shapes, including complicated three-dimensional bodies. von Karman[2] offered one of the earliest treatments. He considered a uniform flow combined with an axial distribution of line sources and sinks to compute the velocity and pressure distributions for a given body shape. Oberkampf and Watson[3] made a comprehensive study of the von Karman approach and found that it produces a nearly ill-conditioned system of simultaneous equations. The method also was found to be sensitive to the number of elements used, the fineness ratio, and the regularity of the body shape. Results were presented for bodies of fineness ratios of 4 and 10.

Smith and Pierce[4] treated the direct problem in terms of surface-distributed singularities. The surface distributions lead to a Fredholm integral equation of the second kind, which can be represented by a system of linear algebraic equations. This approach has had numerous extensions, most notably by workers at the McDonnell-Douglas Corporation. Hess and Smith[5] and Hess[6-9] have made considerable advances in improving the accuracy and extending the capabilities of the method. They extended the earlier work of Smith and Pierce to three-dimensional bodies of arbitrary shape. The primary purpose of these extensions was for aircraft design, although the techniques certainly are applicable to any submerged body.

Parsons, Goodson, and Goldschmied[10] used the Douglas-Neumann method, together with a boundary-layer-drag calculation scheme, for shaping axisymmetric bodies for minimum drag. They represented hull shapes in terms of eight parameters. By use of a computer-oriented optimization procedure, they were able to find a body shape that produced a drag coefficient one-third less than the best previously available laminar flow design. Since the body shapes were prescribed in advance, the method was based on the solution of the direct problem. Grodtkjaer[11] and Webster[12] also have used the surface-source approach in describing solutions to the direct problem. Grodtkjaer computed velocity distributions for ellipsoids of revolution and obtained excellent comparisons to results of Hess and Smith[5] and to existing and analytical solutions. Webster extended the method of Hess and Smith by using triangular surface elements and letting the source strength vary linearly across the element. He produced results that converged more rapidly and with better accuracy than the Douglas program.

The inverse problem has received much less attention in the literature in comparison to the direct problem. Solutions to the inverse problem are admittedly of a crude nature. It is not known in advance whether a given pressure distribution uniquely determines a body shape.

The first approach to the determination of a body shape to meet a prescribed velocity or pressure distributions was by Young and Owen (see Thwaites[13]). They used a perturbation velocity approach; their work later was found to be related to the slender body approximation, and thus did not hold for low fineness ratios; nor did it work well at the leading and trailing edges. McNown and Hsu[14] later developed essentially the same inverse method, and their results showed the same tendencies as those of Young and Owen. Marshall[15] presents the inverse problem as the "design problem in hydrodynamics." He defines a "development problem" as one in which a slight known change in surface pressure distribution produces a to-be-determined slight change in body shape. This development problem is a step or a sub-problem in the design problem. A perturbation technique was used to transform the free boundary problem into a well-posed problem, which was solved numerically, using techniques of the Douglas program. The procedure is necessarily iterative. Marshall applied his technique to two ellipsoids of revolution of slightly different thickness ratios (0.968 and 0.971). With 77-point subdivision of the x axis, the maximum error in calculated body shape reached 15% for the nose and tail regions, whereas, for the remainder of the body, the error amounted to less than 2%.

Bristow[1] treated the inverse problem using the Douglas program. An iterative method was developed in which the body geometry is updated such that the mean-square difference between the prescribed and calculated velocity distributions is minimized. The procedure is not strongly dependent on the starting body geometry, and convergence was attained usually after 5 to 10 iterations. Bristow's approach probably is the most comprehensive and accurate treatment to date of the inverse problem. However, the procedure is based on an approximate, but complex, relationship between the velocity perturbations and geometry perturbations. Bristow presented results for three cases and obtained excellent agreement, either between calculated and exact geometries or between prescribed and calculated velocity distributions. Ten iterations were necessary to obtain such excellent results.

III. Mathematical Description

The present method for solving the inverse problem is based on the idea of axial source distribution, which has been presented by several authors, e.g., Robertson[16] and Karamcheti.[17] Figure 1 shows the basic arrangement of line source and sink elements, combined with a uniform flow to produce the body of revolution. The relation between the coordinates ξ, η and x, r is given by $\xi = x - x_j$ and $\eta = r$, where x_j is the leading edge coordinate of the jth element. The stream function, due to an element j at an arbitrary point ξ, η, is given by (see Eskinazi[18])

$$\psi_j(\xi,\eta) = (m_j/4\pi)\left[\sqrt{(\xi-\ell_j)^2+\eta^2} - \sqrt{(\xi^2+\eta^2)}\right]$$

This can be written in the coordinate system x, r as follows:

$$\psi_j(x,r) = (m_j/4\pi)\left[\sqrt{(x-x_j-\ell_j)^2+r^2} - \sqrt{(x-x_j)^2+r^2}\right] \quad (1)$$

The velocity components in x and r directions are given by

$$u = (1/r)(\partial\psi/\partial r)$$

and

$$v = -(1/r)(\partial\psi/\partial x)$$

This gives the following expressions for u and v at an arbitrary point (x,r) due to an element j,

$$u_j(x,r) = \frac{m_j}{4\pi}\left[\frac{1}{\sqrt{(x-x_j-\ell_j)^2+r^2}} - \frac{1}{\sqrt{(x-x_j)^2+r^2}}\right] \quad (2)$$

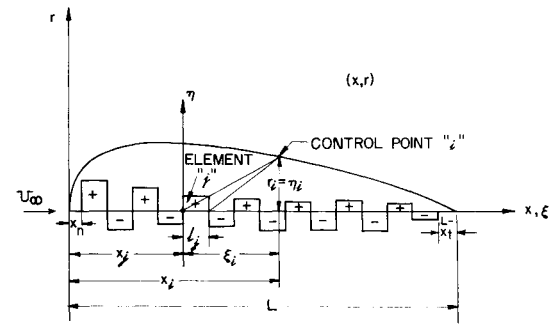

Fig. 1 Definition sketch of elements.

and

$$v_j(x,r) = \frac{-m_j}{4\pi r}\left[\frac{(x-x_j-\ell_j)}{\sqrt{(x-x_j-\ell_j)^2+r^2}} - \frac{x-x_j}{\sqrt{(x-x_j)^2+r^2}}\right] \quad (3)$$

The stream function and velocity components at a control point i, due to an element j of unit strength, are

$$\bar{\psi}_{ij} = \frac{1}{4\pi}\left[\sqrt{(x_i-x_j-\ell_j)^2+r_i^2} - \sqrt{(x_i-x_j)^2+r_i^2}\right] \quad (4)$$

$$\bar{u}_{ij} = \frac{1}{4\pi}\left[\frac{1}{\sqrt{(x_i-x_j-\ell_j)^2+r_i^2}} - \frac{1}{\sqrt{(x_i-x_j)^2+r_i^2}}\right] \quad (5)$$

and

$$\bar{v}_{ij} = \frac{-1}{4\pi r_i}\left[\frac{(x_i-x_j-\ell_j)}{\sqrt{(x_i-x_j-\ell_j)^2+r_i^2}} - \frac{(x_i-x_j)}{\sqrt{(x_i-x_j)^2+r_i^2}}\right] \quad (6)$$

Superposing the stream function and velocities of the uniform flow to those of the source-sink distribution, the total flowfield at a control point i is obtained:

$$\psi_i = \sum_{j=1}^{N_e} m_j\bar{\psi}_{ij} + U_\infty r_i^2/2 \quad (7)$$

$$u_i = \sum_{j=1}^{N_e} m_j\bar{u}_{ij} + U_\infty \quad (8)$$

$$v_i = \sum_{j=1}^{N_e} m_j\bar{v}_{ij} \quad (9)$$

where N_e is the number of elements.

The direct problem was solved by von Karman[2] by equating ψ_i to zero at a number of control points equal to the number of elements. Solution of the resulting system of linear equations yields the strength m_j of each element.

IV. The Inverse Problem

The inverse problem may be treated as follows: Given the surface velocity distribution $Q_i = q_i/U_\infty$ at a number of points along the body axis, find the contour points $R_i = r_i/L$ which define the body shape. The solution of such a problem has been achieved by using the tangency condition together with Eqs. (7-9), which usually are used to solve the direct problem. Of course the tangency condition $[dr/dx = v/u]$ and the equation $\psi = 0$ on the body surface are equivalent; however, the use of both of them through the strategy discussed in the following enabled us to develop the iterative scheme to find the body geometry.

Method of Solution

The present method starts with an initial guess of the body geometry. This initial guess can be very crude. First, the velocity component u_i is calculated from the given total

velocity distribution q_i by applying the tangency condition (i.e., the total velocity is everywhere tangential to body surface) to the starting geometry. With the starting geometry, the matrices $\bar{u}_{ij}$, $\bar{v}_{ij}$, and $\bar{\psi}_{ij}$ can be constructed; then the system of Eqs. (8) is solved for the source intensities m_j. An improved geometry then can be obtained by solving Eq. (7) for r_i with the values of m_j just obtained, and with $\psi_i = 0$ on the body surface. This new contour replaces the initial guess, and the same computational sequence is repeated until convergence is obtained.

Numerical Scheme

The governing equations are first put into dimensionless form; Eqs. (7-9) become

$$\sum_{j=1}^{N_e} M_j \bar{U}_{ij} = U_i - 1 \tag{10}$$

$$\sum_{j=1}^{N_e} M_j \bar{V}_{ij} = V_i \tag{11}$$

and

$$R_i = \sqrt{-2 \sum_{j=1}^{N_e} M_j \bar{\Psi}_{ij}} \tag{12}$$

with

$$M_j = m_j / U_\infty L \qquad \bar{U}_{ij} = \bar{u}_{ij} L \qquad \bar{V}_{ij} = \bar{v}_{ij} L$$

$$R_i = r_i / L \qquad \bar{\Psi}_{ij} = \bar{\Psi}_{ij} / L \qquad U_i = u_i / U_\infty$$

In order to apply the tangency condition, one needs to determine the slopes of the contour at point i. A parabola is passed through the point i, and the two adjacent points, $i-1$ and $i+1$. By use of Lagrange's method, the slope at point i is

$$S_i = R_{i-1} \frac{(X_i - X_{i+1})}{(X_{i-1} - X_i)(X_{i-1} - X_{i+1})} + R_i \frac{(2X_i - X_{i-1} - X_{i+1})}{(X_i - X_{i-1})(X_i - X_{i+1})} + R_{i+1} \frac{(X_i - X_{i-1})}{(X_{i+1} - X_{i-1})(X_{i+1} - X_i)} \tag{13}$$

where $X_i = x_i / L$.

The numerical scheme is described as follows:

1. Assume a starting body geometry,

$$R_i^\circ = f(X_i)$$

(An ellipsoid of arbitrary thickness proved to be a good starting shape.)

2. The slope S_i of the profile is calculated at each control point i using Eq. (13).

3. The axial velocity component U_i is calculated by applying the tangency condition, and using the slopes determined in the previous step and the prescribed velocity distribution Q_i:

$$U_i = \frac{Q_i}{\sqrt{1 + S_i^2}} \tag{14}$$

4. The three matrices $\bar{\Psi}_{ij}$, $\bar{U}_{ij}$, $\bar{V}_{ij}$, which are functions of the geometry of the profile, are evaluated.

5. With the values of U_i determined in step 3, and $\bar{U}_{ij}$ determined in step 4, Eqs. (10) are solved for the values of the source intensities M_j.

6. With the values of M_j determined in step 5, and $\bar{\Psi}_{ij}$ in step 4, the new body coordinates R_i are calculated using Eq. (12).

7. Steps 2-6 now are repeated with the new R_i values until convergence is obtained.

Convergence Criteria

There are three possible criteria by which convergence may be judged:

1. When the rms value of the difference between the body coordinates R_i in two successive iterations

$$\text{rms})_R = \sqrt{\frac{1}{Ne} \sum_{i=1}^{N_e} (R_i^{(k+1)} - R_i^{(k)})^2} \tag{15}$$

is less than a small quantity ϵ_1.

2. When the calculated velocity distribution is essentially the prescribed one. The magnitude of the total velocity is

$$Q_{i,\text{calc}} = \sqrt{U_i^2 + V_i^2} \tag{16}$$

where U_i is obtained from Eq. (14) and V_i from Eq. (11). The difference between the prescribed and calculated velocity distributions may be represented by

$$\text{rms})_Q = \left[\frac{1}{N_e} \sum_{i-1}^{N_e} (Q_{i,\text{calc}} - Q_{i,\text{presc}})^2 \right]^{1/2} \tag{17}$$

When $\text{rms})_Q \leq \epsilon_2$, the solution can be considered to have converged.

3. When the ratio V_i / U_i compares favorably to the slope of the contour S_i, the solution is accepted. The velocities V_i and U_i are obtained as described in Criterion 2.

Application of these three convergence criteria to a number of test cases indicated that Criterion 2 is the best. Criterion 1 should not be applied alone, since it produced acceptable body shapes that were different from the exact profiles. This happened in some test cases when a small number of elements was used, or when the convergence was slow. Criterion 3 proved to be a good one, except near the nose and tail, where there is more uncertainty in the calculated slopes. However, this criterion gave a good view of how the calculated geometry is compatible with the tangency condition in each iteration. The values of ϵ_1 and ϵ_2 used, in most cases, were 0.001 and 0.03.

Comments on the Numerical Scheme

1. Double precession calculations were used in the formation of the matrices $\bar{U}_{ij}$, $\bar{V}_{ij}$, and $\bar{\Psi}_{ij}$.

2. The system of linear equations in each iteration was solved by Gaussian elimination with scaling and pivoting.

3. Elements of equal sizes were used,

$$\ell_j = (x_t - x_n) / N_e = \text{const}$$

where x_n is the point at which the distribution starts, x_t is where it ends, and N_e is the number of elements included (see Fig. 1). The number of elements necessary for accurate solutions ranged from 18 for a sphere to 44 for bodies of fineness ratio 10.

4. The control points on the body contour were chosen at an x value corresponding to the middle of each element. This excluded the leading and trailing edges as control points.

5. In order to have a closed profile, the net efflux of sources and sinks should be zero,

$$\sum_{j=1}^{N_e} M_j \ell_j = 0 \tag{18}$$

Since Eq. (18) represents a strong requirement, it was used instead of one of the equations in the system (10). It usually replaced the equation corresponding to a control point in the middle of the profile. It was found that inclusion of Eq. (18) improved the condition of the matrix substantially. Adding

Eq. (18) to each equation removed the diagonal zeros of the matrix $\bar{U}_{ij}$. The use of Eq. (18) reduced the errors in the solution of equations to an order of 10^{-8}.

6. In step 3 of the numerical scheme, V_i could have been calculated instead of U_i:

$$V_i = S_i Q_i / \sqrt{1+S^2} \tag{19}$$

and in step 5, M_j would be obtained by solving Eqs. (11). This variation was attempted, and convergence was found to be slow compared to the stated procedure. A second variation was to alternate the solution procedure between the U_i and V_i calculations in successive iteration rounds. This variation produced convergence, but also was at a slower rate than the preferred procedure, i.e., using U_i equations only to determine M_j.

7. Since the leading and trailing edges of the body were excluded as control points, the starting and ending points of the singularity distributions x_n and x_t were taken as the leading and trailing stagnation points, respectively, i.e., $x_n = 0$ and $x_t = L$. This choice is made so that the control points cover the entire contour. Oberkampf and Watson[3] used the same selection. In several cases, we offset x_n and x_t from the stagnation points ($x_n = 0.02L$ and $x_t = 0.98L$). The effect of these values on the results was negligible.

8. The solution of the inverse problem presented in this paper was relatively more successful as compared to the solution of the direct problem using the same concept of axial source/sink distribution. This is because, in solving the direct problem, the source strengths are obtained by solving the system of Eqs. (7) with $\psi_i = 0$ on the body surface. In solving the inverse problem, such strengths are obtained by solving a different system of equations, given here by Eq. (8).

As for the direct problem, our numerical experiments for the case of a sphere showed that the matrix $\bar{\psi}_{ij}$ is ill-conditioned in general. Moreover, evaluation of the matrix elements involve subtraction of nearly equal quantities $(\sqrt{(x_i - x_j - \ell_j)^2 + r_i^2}$ and $\sqrt{(x_i - x_j)^2 + r_i^2}$ become very close as the ℓ_j becomes smaller, i.e., the number of elements becomes larger). This introduces round-off error, which may cause the solution of the ill-conditioned system to blow up. The relative round-off error in the evaluation of the elements can be minimized by scaling the body coordinates by a small reference length. The element length seems to be a good choice (von Karman[2] and Oberkampf and Watson[3]) since it decreases as the number of elements increase. Our numerical experiments showed that, with double-precision calculations on the Univac 1108, the solution blows up for $N_e \geq 12$ when normalizing by the body length. On the other hand, when normalizing by the element length, the solution was possible for a number of elements of 20.

For the inverse problem, the matrix $\bar{u}_{ij}$ is equal to the difference between the reciprocals of the terms of $\bar{\psi}_{ij}$. Thus, in order to reduce the round-off error in subtraction, one has to use a large reference length for normalization. By doing so, the numerical value of $1/\sqrt{(x_i - x_j - \ell)^2 + r^2}$ and $1/\sqrt{(x_i - x_j)^2 + r^2}$ is increased.

We used the body length for normalization, and results were quite good. Recently, we carried out a numerical experiment using the element length for scaling instead of L; the solution always blows up and divergence occurs early in the iteration procedure. Also based on our numerical experiments, we can say that the solution of the system (8) (the inverse problem), when coordinates are scaled by L, is more stable than system (7) (the direct problem) when coordinates are scaled by the element length ℓ.

V. Test Cases

The algorithm described in Sec. IV has been programmed on the Univac 1108 digital computer. Several example problems have been selected to illustrate the method.

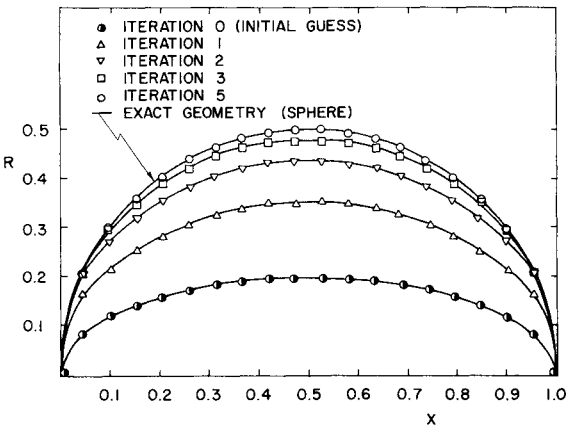

Fig. 2 Body profiles for a sphere.

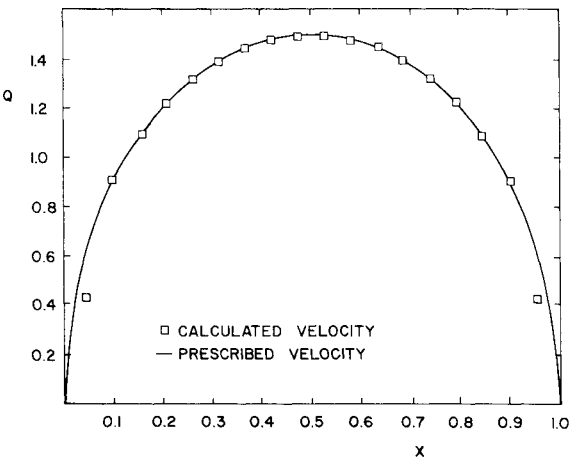

Fig. 3 Velocity distributions for a sphere.

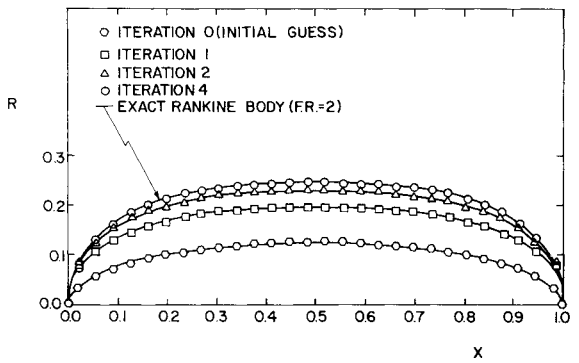

Fig. 4 Body profiles for a Rankine body of fineness ratio 2.

Case 1 – Flow around a Sphere

The velocity distribution for potential flow around a sphere is given by

$$Q_i = 3/2 \sin\theta$$

or

$$Q_i = 3\sqrt{X(1-X)}$$

where X is measured from the nose along the axis of symmetry. With this velocity distribution, the computations were performed for two different numbers of elements, 12 and 18. As was stated earlier, convergence was better for the larger number. The discussion from here on for the sphere results will refer to the 18 element case. Figure 2 shows the initial

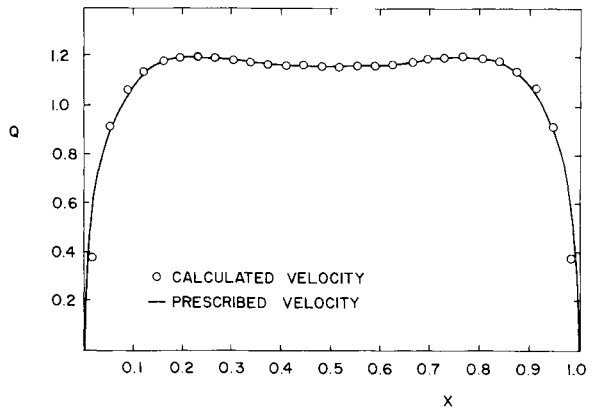

Fig. 5 Velocity distributions for a Rankine body of fineness ratio 2.

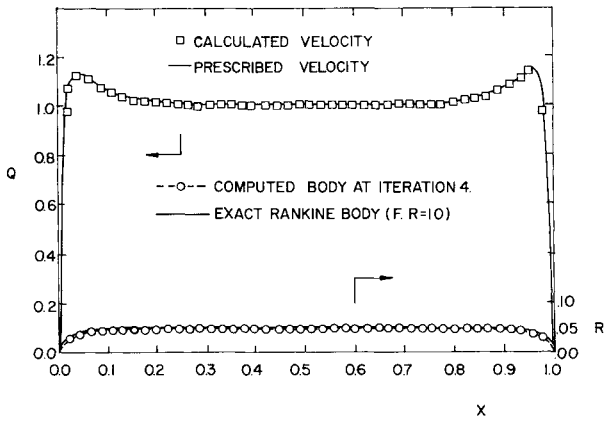

Fig. 6 Body profiles and velocity distributions for a Rankine body of fineness ratio 10.

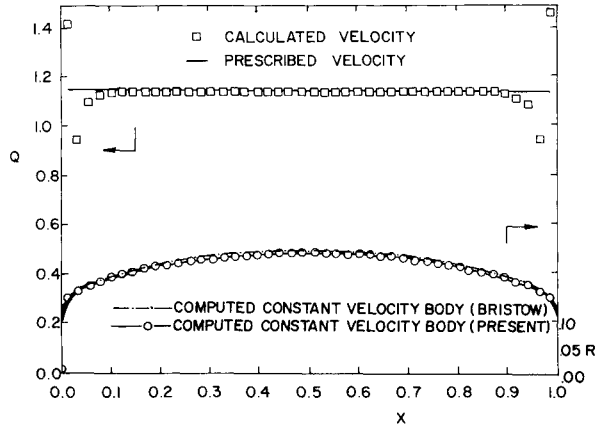

Fig. 7 Body profiles and velocity distributions for a constant velocity body.

(assumed) profile and the profiles at the various iteration levels. Convergence on the body shape was attained in five iterations. The converged geometry agrees very well with the spherical shape. A comparison between the computed velocity distribution of the converged geometry and the prescribed velocity distribution is shown in Fig. 3. Agreement between velocities is quite good except near the stagnation points. The inaccuracy near these points is due to the uncertainty in the computation of the slope.

Case 2 – Flow around an Axisymmetric Rankine Body

Axisymmetric Rankine bodies of fineness ratios 2, 4, and 10 were considered as a test of the method. The coordinates of the body necessary for comparison were obtained by solving

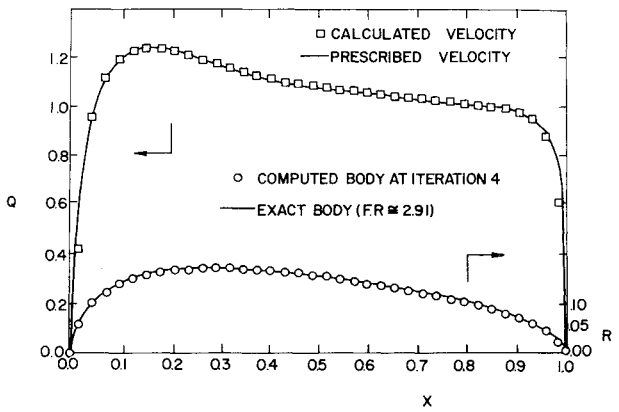

Fig. 8 Body profiles and velocity distributions for an axisymmetric airfoil of fineness ratio 2.91.

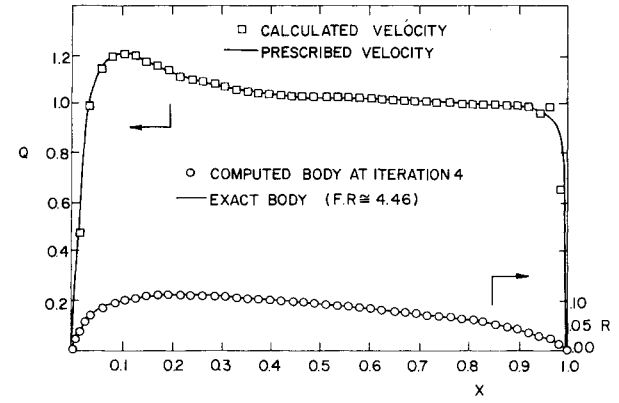

Fig. 9 Body profiles and velocity distributions for an axisymmetric airfoil of fineness ratio 4.46.

the analytic nonlinear body profile (see Eskinazi[18]) by means of the Newton-Raphson method. The velocity input was the exact velocity distribution for each fineness ratio. The initial body shape was taken to be an ellipsoid. The number of elements necessary for accurate solutions in each case was 28, 44, and 44, respectively. The number of iterations necessary for convergence was 4 in all cases.

Figure 4 shows the initial profile and the profiles at the various iterations for a fineness ratio of 2. Figure 5 shows comparison between the calculated and prescribed velocity distributions. Again, agreement is excellent except near the stagnation points for reasons stated in the sphere discussion. For a fineness ratio of 10, results are shown in Fig. 6. The agreement between computed and exact profiles and velocities is not as good as for a fineness ratio of 2, but is still quite good. For a fineness ratio of 4, the comparisons also were excellent, but are not presented graphically.

Case 3 – Constant Velocity Body

The challenging problem of a constant velocity body was the next case attempted to demonstrate our solution to the inverse problem. A velocity distribution of $U/U_\infty = 1.15$ was chosen since Bristow[1] used this same value for a constant velocity body calculation. Figure 7 shows the results of the present method compared to the results of Bristow. Over about 80% of the body length, excellent agreement between prescribed and calculated velocities is noted. Very close to the nose or tail, the differences in velocity are not negligible. Our method produces an overshoot in the velocity close to the nose. Bristow also had the problem of high velocity near the nose and the tail of the body. He overcame this difficulty by modifying the converged geometry to obtain a flat disk nose and tail necessary for sudden change in velocity at these two locations. The flat disk nose and tail then were reduced in size

in order to obtain agreement between prescribed and calculated velocities. No such alterations were attempted using our approach; we still obtained fair agreement with Bristow's results, except at points very near the nose and tail. Our calculations were done using 44 elements.

Case 4 – Axisymmetric Airfoil-Type Shape

An axisymmetric airfoil-type shape may be obtained by combining a uniform flow, a point source, and a line sink (Robertson[16]). The exact velocity distribution for such a body with fineness ratio of 2.91 was calculated, and input to the program and results are shown in Fig. 8. Excellent agreement between the exact and computed body shapes was obtained by using 36 elements. The computed and the prescribed velocity distributions also are noted to be in excellent agreement. Results also were obtained for a body of fineness ratio 4.46. With 44 elements, very good agreement also was obtained, as shown in Fig. 9.

VI. Possible Extensions

The first of several different variations would be to improve the accuracy of the method by means of a linear variation of the source (or sink) strength over the element. Another approach to improving the accuracy of the method would be in terms of a continuous distribution of sources and sinks over the axis of the body. In this latter case, no elements would be used; the distribution is represented by a polynomial or Fourier series, with a number of unknown coefficients to be determined by use of the given velocity distribution. Either of the two approaches should allow the computation time to be cut substantially and the accuracy to be improved. Further investigation on these two improvements is currently under consideration.

VII. Conclusions

An algorithm that is simple, concise, fast, and accurate has been developed to solve the inverse problem in hydrodynamics. The method is iterative, and is based on representing bodies of revolution in axisymmetric flow by a distribution of line sources and sinks along the axis with possible inclusion of a point source or sink. The iterative scheme was made possible by the use of two equivalent conditions using a certain strategy: the tangency condition in the form $dr/dx = v/u$, and the condition $\psi = 0$ on the body surface. Rapid convergence was obtained for all examples considered; four to five iterations were sufficient to provide accurate solutions. The use of the closure condition to replace one equation of the system of linear equations [Eq. (10)] improved the conditioning of the coefficient matrix. Comparison was made to the method of Bristow when possible. The present method converged in fewer iterations with a much more simple computational procedure in each iteration. However, our method cannot deal with bodies of irregular surfaces. The algorithm outlined in this paper should be of inestimable value in the computation of low drag shapes such as torpedoes, submarines, airships, and other axisymmetric, fully submerged bodies.

References

[1] Bristow, D. R., "A Solution to the Inverse Problem for Incompressible Axisymmetric Potential Flow," presented at the AIAA Fluid Dynamics Conference, Palo Alto, Calif., June 1974.

[2] von Karman, T., "Calculation of the Flowfield around Airships," NACA TM 574, July 1930.

[3] Oberkampf, W. L. and Watson, L. E., "Incompressible Potential Flow Solutions for Arbitrary Bodies of Revolution," *AIAA Journal*, Vol. 12, March 1974, p. 409.

[4] Smith, A.M.O. and Pierce, J., "Exact Solution of the Neumann Problem," Douglas Rept. ES 26988, Douglas Aircraft Co., April 1958.

[5] Hess, J. L. and Smith, A.M.O., "Calculation of Potential Flow About Arbitrary Bodies," *Progress in Aeronautical Sciences*, Pergamon Press, New York, 1967, Vol. 8.

[6] Hess, J. L., "Higher Order Numerical Solution of the Integral Equation For the Two-Dimensional Neumann Problem," Computer Methods in Applied Mechanics and Engineering, Vol. 2, 1973, p. 1.

[7] Hess, J. L., "The Problem of Three-Dimensional Lifting Potential Flow and Its Solution by Means of Surface Singularity Distribution," *Computer Methods in Applied Mechanics and Engineering*, Vol. 4, 1974, p. 283.

[8] Hess, J. L., "Review of Integral-Equation Techniques for Solving Potential Flow Problems with Emphasis on the Surface-Source Method," *Computer Methods in Applied Mechanics and Engineering*, Vol. 5, 1975, p. 145.

[9] Hess, J. L., "The Use of Higher-Order Surface Singularity Distributions to Obtain Improved Potential Flow Solutions For Two-Dimensional Lifting Airfoils," *Computer Methods in Applied Mechanics and Engineering*, Vol. 5, 1975.

[10] Parsons, J. S., Goodson, R. E., and Goldschmied, F. R., "Shaping of Axisymmetric Bodies for Minimum Drag in Incompressible Flow," *Journal of Hydronautics*, Vol. 8, July 1974, p. 100.

[11] Grodtkjaer, E., "A Direct Integral Equation Method for the Potential Flow About Arbitrary Bodies," *International Journal of Numerical Methods and Engineering*, Vol. 6, 1973, p. 253.

[12] Webster, W. C., "The Flow about Arbitrary, Three-Dimensional Smooth Bodies," *Journal of Ship Research*, Vol. 19, 1975, p. 206.

[13] Thwaites, B. (ed.), *Incompressible Aerodynamics*, Oxford University Press, Oxford, 1960.

[14] McNown, J. S. and Hsu, E-Y, "Approximation of Axisymmetric Body Forms for Specified Pressure Distributions," *Journal of Applied Physics*, Vol. 22, Oct. 1951, p. 864.

[15] Marshall, F. J., "Design Problem in Hydrodynamics," *Journal of Hydronautics*, Vol. 4, 1970, p. 136.

[16] Robertson, J. M., *Hydrodynamics in Theory and Application*, Prentice Hall, Inc., Englewood Cliffs, 1965.

[17] Karamcheti, K., *Principles of Ideal-Fluid Aerodynamics*, John Wiley & Sons, New York, 1966.

[18] Eskinazi, S., *Vector Mechanics of Fluids and Magnetofluids*, Academic Press, New York, 1967.

Announcement: 1977 Author and Subject Index

The indexes of the five AIAA archive journals (*AIAA Journal, Journal of Aircraft, Journal of Energy, Journal of Hydronautics, Journal of Spacecraft and Rockets*) will be combined and mailed separately early in 1978. In addition, papers appearing in volumes of the *Progress in Astronautics and Aeronautics* book series published in 1977 will be included. Librarians will receive one copy of the index for each subscription which they have. Any AIAA member who subscribes to one or more Journals will receive one index. Additional copies may be purchased by anyone, at $10 per copy, from the Circulation Department, AIAA, Room 730, 1290 Avenue of the Americas, New York, New York 10019. **Remittance must accompany the order.**

Ruth F. Bryans
Director, Scientific Publications